

AN OVERVIEW OF RESEARCH AT NBS USING SYNCHROTRON RADIATION AT SURF-II

D.L. Ederer, R.P. Madden, A.C. Parr, G. Rakowsky, E.B. Saloman
Center for Radiation Research
National Bureau of Standards
Washington, DC 20234

J. Cooper
Center for Absolute Physical Quantities
National Bureau of Standards
Washington, DC 20234

R. Stockbauer and T.E. Madey
Center for Chemical Physics
National Bureau of Standards
Washington, DC 20234

J.L. Dehmer
Argonne National Laboratory
Argonne, IL 60439

Summary

The National Bureau of Standards (NBS) Synchrotron Ultraviolet Radiation Facility (SURF-II) is used in conjunction with several high throughput monochromators to study the interaction of vacuum ultraviolet photons with solids and gases. Recent work has been concerned with the photon stimulated desorption of atomic and molecular ions from surfaces, with the effect of electric fields on molecular photoabsorption and with the study of molecular photoionization by angle resolved photoelectron spectroscopy. These research programs yield new information about molecular bonding at surfaces, molecular dynamics near ionization thresholds, and the coupling of the electronic and nuclear motion near resonances in molecules. In addition to these programs in basic research SURF-II is used for the calibration of transfer standard detectors over a photon energy range 20-250 eV. Calibration of monochromator systems is achieved over the photon energy range 5-250 eV by using the now calculable spectral intensity radiated by the electrons, which are confined in a nearly circular orbit.

Introduction

This paper is a description of the major programs at the Synchrotron Radiation Facility at the National Bureau of Standards, SURF-II. The programs at SURF-II are divided into four areas: 1] Radiometry, 2] Solid State and Surface Physics, 3] Atomic and Molecular Physics and 4] Machine Improvement. The facility has, as a source of radiation, an electron storage ring which recently has been upgraded to 280 MeV. The electrons orbit in an almost perfect circle of radius 84 cm. The continuum spectral distribution of the radiation for several electron energies is shown in Fig. 1.

Although the spectral distribution of the radiation from SURF-II extends from the infrared to the soft x-ray region, the instrumentation located at SURF-II is designed primarily for the wavelength region 5-250 eV (200-4 nm). This spectral region requires evacuated spectrometers and beamlines. Ultrahigh vacuum ($p < 5 \times 10^{-9}$ Torr) must be maintained in the beamlines,

ring vacuum chamber, and spectrometers to keep the optical surfaces from being contaminated and to insure electron beam lifetimes of several hours. However, in some of the gas phase experiments, pressures of up to 10^{-4} Torr can be used when adequate differential pumping is provided to maintain the ring at ultrahigh vacuum.

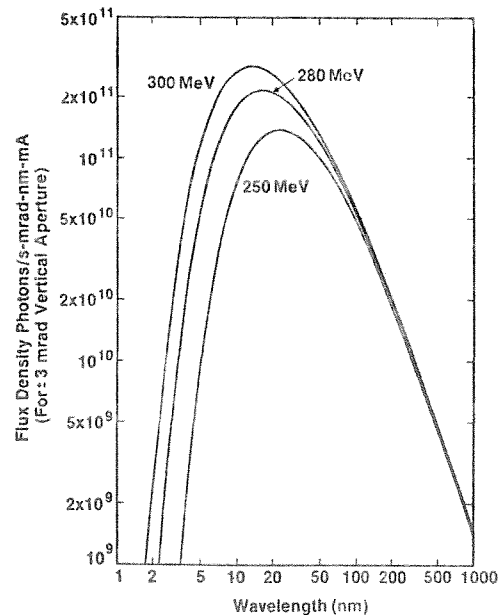


Fig. 1. Spectral distribution of synchrotron radiation sources as a function of electron energy.

A schematic diagram of the SURF-II facility is shown in Fig. 2. Of the eleven beamlines, seven are in use and two more will be commissioned in 1983. The radiometric efforts are concentrated mainly on beamline 2, (BL-2), 3, 9, 10, and 11. The solid state experiments are on beamline 8, (BL-8); the atomic and molecular physics experiments are carried out primarily on BL-3 and BL-5. Since the last report¹ several improvements to the facility have been made or are in the process of being installed. In addition to increasing the electron kinetic energy from 250 MeV to 280 MeV, the accelerator staff is working on upgrading the injector output so that higher currents can be stored. Two new monochromators are under construction. One is a high-throughput toroidal grating monochromator² (TGM) and is slated for installation on BL-1 in the early part of 1983. This monochromator will accept up to 50 mrad of the horizontal output of the ring and covers the wavelength range 8-60 nm (150-20 eV). The other monochromator is also a TGM. It will be mounted on BL-10 and will be used primarily to calibrate transfer standard diodes³ in the XUV. Both instruments are expected to have a source limited bandpass of about 30 meV. These instruments use the high brightness electron beam (0.1 mm high and 1.5 mm wide) from SURF-II directly as the entrance slit. They complement the high-throughput normal-incidence monochromator⁴ presently installed on BL-5.

Radiometric Program

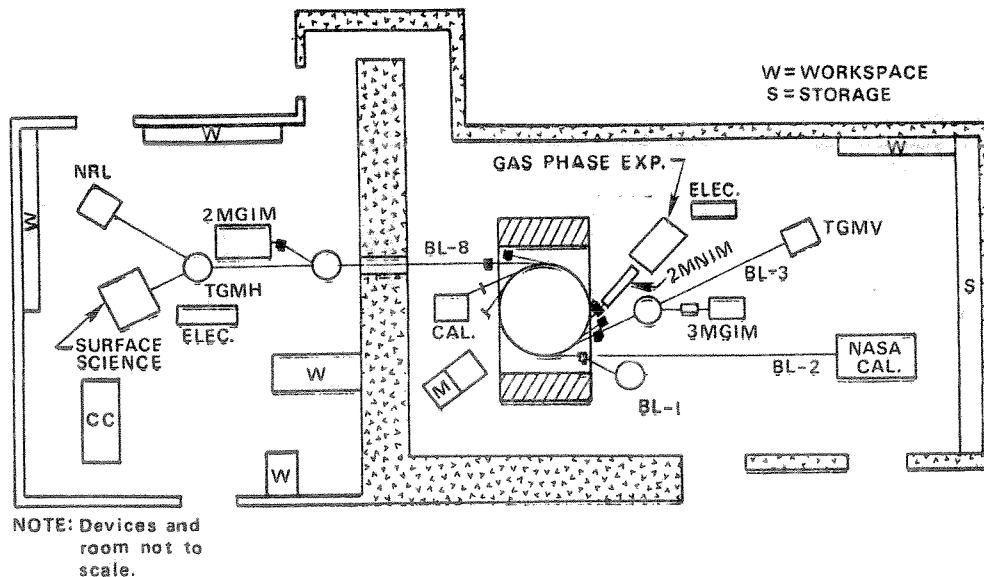
SURF-II is a unique source for radiometry. The storage ring at SURF-II is the only one in the world where the orbit is circular. (This facilitates the determination of the orbital radius and the location of the source of radiation.) The magnetic field has been carefully characterized and the total energy of the electrons and their radius are measured to an accuracy of 0.1%. This enables one to calculate the flux per electron, using classical theory.⁵ If the electron current can be determined with suitable

accuracy, one can calibrate the efficiency of spectrometers placed in the beam. By the use of electron counting,⁶ the sensitivity of a highly linear silicon diode is calibrated in the range of 10 to 10³ circulating electrons and then this detector is used, by means of its linearity to measure currents ranging from 10⁸-10⁹ circulating electrons (corresponding to a beam current 1-10 mA). By this technique, it is possible to determine the electron beam current with an accuracy of 1.7%. With future improvements, we expect to determine the beam current to about 0.2%. The expected calibration accuracy obtainable at several wavelengths is shown in Table 1.

NASA has provided support for the construction of a spectrometer calibration facility at SURF-II. A schematic of the system⁷ is shown in Fig. 3. The large optical calibration chamber can be translated in two directions to scan the synchrotron beam over an optical element. A gimbal is mounted inside the tank. This device can be rotated in two directions, providing the capability of scanning an instrument about a fixed point of rotation. Thus, if a spectrometer is mounted

Table 1. Error budget in the use of SURF-II as an absolute source of irradiance. Wavelength units 1 nm = 10Å.

Determination of Orbital Current	1.7%
Energy of Orbiting Electrons	2.5%(4 nm)-0.04%(200 nm)
Orbital Radius	< 0.5%
Beam Position	< 0.1%
Finite Source Size	< 0.1%
Precision of Calculated Model	< 0.1%
Scattered Light	< 1.0%
Total Systematic Error	3.2%(4 nm)-2.0%(200 nm)
Random Errors	< 1.0%



Schematic of Beamlines at SURF-II

Fig. 2. Schematic floor plan for the SURF-II facility. TGMV is a toroidal grating monochromator with dispersion in the vertical plane. 2MGIM and 2MGIM are 3 and 2 m grazing incidence monochromators, respectively. TGMH is a toroidal grating monochromator with dispersion in the horizontal plane, while HFNIM is a 2 m high-flux normal-incidence monochromator.

on the gimbal with its entrance slit on the point of rotation, the synchrotron beam can be used to map out the efficiency of the optical elements in the spectrometer. For example, this calibration chamber is being used to characterize SUSIM, a spectrometer designed to be used on the space shuttle to observe the irradiance from the sun in the vacuum ultraviolet spectral region. There is another translation-rotation mount available on BL-2 for spectrometers that have vacuum jackets.

NBS also maintains a detector calibration facility mounted on BL-3. The synchrotron radiation continuum is monochromatized by the toroidal grating monochromator and the flux of monochromatized radiation is determined with a double ion chamber.⁸ The ion chamber is replaced by a photodiode standard detector and its efficiency is determined as a function of wavelength from a knowledge of the output photocurrent for a given input photon flux. The efficiency of typical diodes as a function of wavelength λ is shown in Fig. 4. About thirty diodes each year are distributed to government agencies, universities and industry.

Solid State and Surface Physics

The solid state and surface science program is carried out primarily on BL-8. One aspect of the program is run in collaboration with NASA. The reflectivity of mirror materials for use in NASA projects are being characterized in the spectral region between 8 nm and about 32 nm using the monochromator and reflectometer (2MGIM) shown in Fig. 2. Reflectance measurements for chemical vapor deposited silicon carbide⁹ are shown in Fig. 5 as a typical example of the capability of this apparatus.

Tunable radiation in the energy range 25-75 eV is provided by another toroidal grating monochromator (TGMH in Fig. 2) on BL-8. The monochromatic radiation is used to study photon stimulated desorption (PSD) of adsorbed layers from ultraclean substrates. The ultrahigh vacuum chamber attached to the exit slit of TGMH contains a double pass electron energy analyzer, a coolable sample manipulator, optics for low energy electron diffraction (LEED) and electron stimulated desorption ion angular distribution (ESDIAD) measurements, and an ion sputter gun for cleaning crystals. The method of PSD has been reviewed by Madey et al.¹⁰ The technique has developed into a powerful tool to study ionically and covalently bonded systems adsorbed on a substrate.

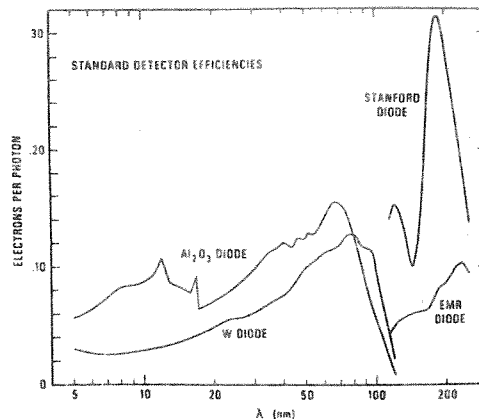


Fig. 4 Photoefficiency of several typical standard detectors as a function of incident wavelength. Wavelength units 1 nm = 10Å.

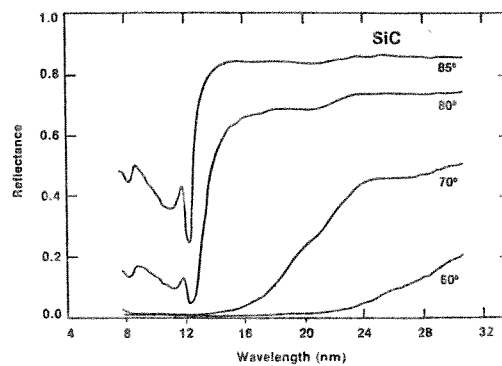


Fig. 5. Reflectance measurements at several angles of incidence for CVD-SiC taken at the NBS Synchrotron. Data is taken from Ref. 9.

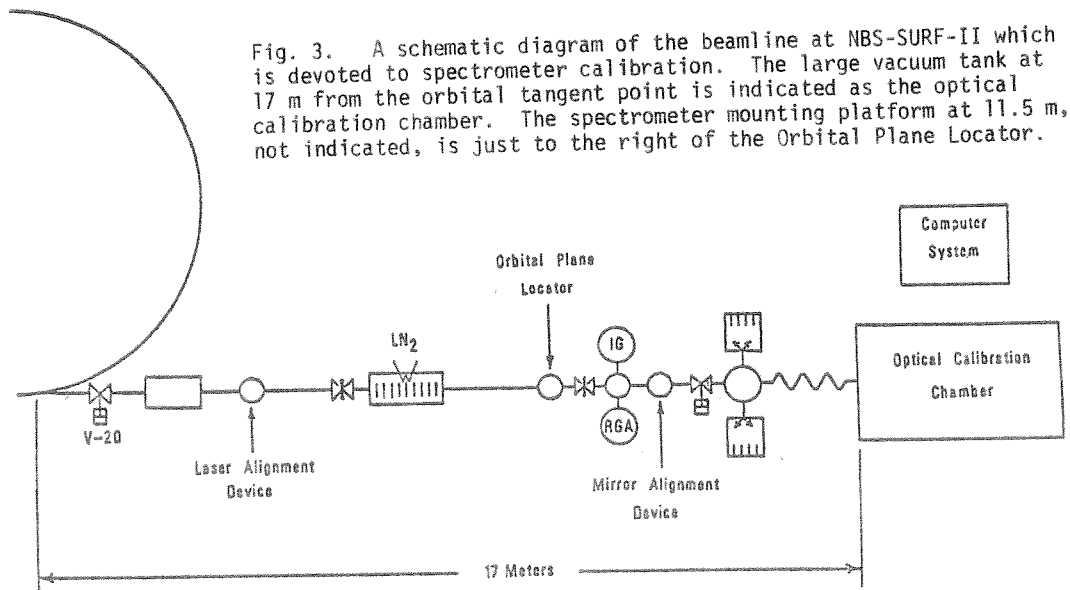


Fig. 3. A schematic diagram of the beamline at NBS-SURF-II which is devoted to spectrometer calibration. The large vacuum tank at 17 m from the orbital tangent point is indicated as the optical calibration chamber. The spectrometer mounting platform at 11.5 m, not indicated, is just to the right of the Orbital Plane Locator.

As an example of the technique, some results¹¹ are presented of photon stimulated desorption of ions from OH and methanol (CH₃OH) adsorbed on a Ti(0001) surface. For this system, the PSD for OH and methanol show quite different behaviors. This is illustrated in Fig. 6, where the H⁺ yield as a function of photon energy is shown for these systems. The lower curve shows the secondary electron yield of titanium, and clearly shows the onset of ionization from the 2p subshell of titanium. The H⁺ onset for CH₃OH seems to be correlated with a 4a' molecular orbital which has a binding energy of about 18 eV. Isotopic labeling shows that H⁺ is emitted almost exclusively by the C-H bond rupture rather than O-H bond rupture. On the other hand, desorption of H⁺ from OH shows a threshold at about 25 eV which is probably associated with the 2s ionization threshold of O at about 25 eV. The enhancement of the yield at 45 eV correlates well with the 2p ionization of titanium. This work is one illustration of the power of PSD as a tool to aid in understanding the nature of covalent bonding of species adsorbed on substrates.

The spectrum emitted by the storage ring at SURF-II falls in one of the windows useful for the fabrication of VSLI masks by lithography. In a cooperative program between NBS and the Naval Research Laboratory, a facility has been developed¹² to study the use of synchrotron radiation to produce ministructures by lithographic techniques. The spectral region between 100 eV and the carbon K edge at 284 eV has been used to expose PBS resist (poly-butene-1-sulfone) and COP, a negative copolymer electron/x-ray resist. Exposure times were approximately 2 minutes for PBS and 8 minutes for COB.

Atomic and Molecular Physics

The program in atomic and molecular physics has centered around a high-resolution grazing-incidence monochromator (3MGIM in Fig. 2) on BL-3, and a high throughput monochromator (2MNIM in Fig. 2) on BL-5. One aspect of the program has been the determination of accurate cross sections in metal vapors,¹³ and the measurement of field effects on high Rydberg series members in the rare gases. Fig. 7 illustrates¹⁴ the role the Stark effect plays in mixing levels and the oscillator strength among high Rydberg series members due to $1s^1S_0 \rightarrow 1s np^1P$ transitions helium. A simple theory due to Foster¹⁵ was used in the diagonalization of the energy matrices. The set of energy levels and their oscillator strengths for a specific principal quantum number was convoluted with the window function of the monochromator to produce the theoretical spectra shown in Fig. 7. The theoretical results are valid for principal quantum numbers, n , less than about 12, where the energy levels from two adjacent values of n begin to overlap. The results for theory and experiment are in good agreement for transitions between the magnetic sublevels $\Delta m=0$ and $\Delta m=1$.

The other aspect of this program deals with the study of the effects produced by resonances on molecular and atomic photoionization. This work has been reviewed recently.¹⁶ The high-throughput normal-incidence monochromator on BL-5 (typical fluxes were 5×10^{10} ph/s-Å) was coupled to an angle resolved photoelectron spectrometer with a resolution of 0.12 eV. In these measurements, the signal, $N_i(\lambda, \theta)$, at a wavelength λ can be expressed in terms of the partial photoionization cross section for the i th channel, $\sigma_i(\lambda)$, and the angular asymmetry parameter $\beta_i(\lambda)$. The equation has the following form:

$$N_i(\lambda, \theta) = K \frac{\sigma_i(\lambda)}{4\pi} \left(1 + \frac{\beta_i(\lambda)}{4} [3p \cos(2\theta) + 1] \right).$$

The quantity K is a proportionality constant related to the geometry of the interaction region and the gas

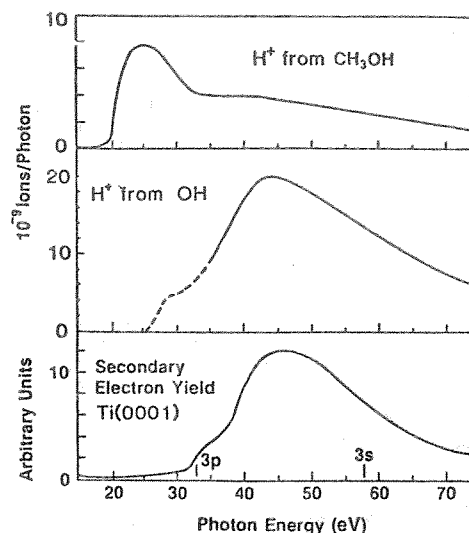


Fig. 6. Comparison of H⁺ yield as a function of photon energy for OH and methanol on Ti(0001). The lower curve shows the secondary electron yield of titanium.

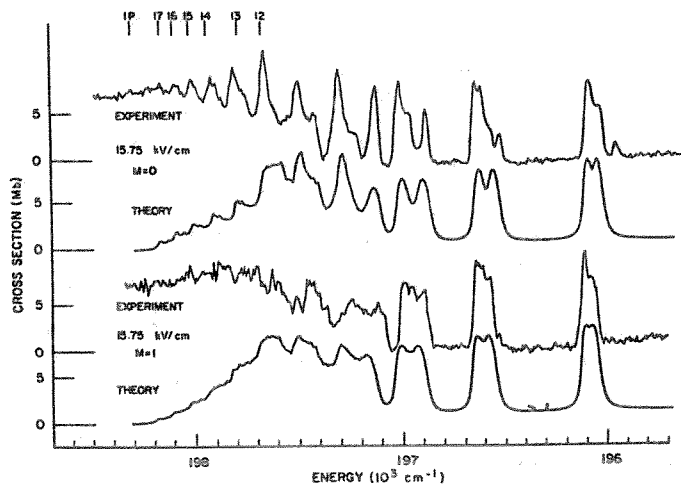


Fig. 7. Comparison of apparent cross sections for a field strength of 15.75 kV/cm with the model calculations. Positions of the highest-energy components of the higher manifolds are shown at the top of the figure.

pressure. The quantity p is the polarization of the radiation and θ is the angle between the emission direction of the electron and the polarization. By measuring $N_i(\lambda, \theta)$ at several angles, $\beta_i(\lambda)$ and a relative value of $\sigma_i(\lambda)$ can be obtained. The absolute value of $\sigma_i(\lambda)$ can be obtained by normalizing the sum of the relative cross section for each channel to the total photoionization cross section at wavelength λ . The variation of $\sigma_i(\lambda)$ and $\beta_i(\lambda)$ can be tracked through the region of an autoionizing resonance, for example, and the dynamics of the photoionization process can be studied. These experiments have been carried out for a large group of molecules. In particular, the diatomics: O₂,¹⁷ N₂,¹⁸ CO,¹⁹ and larger molecules such as SF₆²⁰ have been studied.

As an example of this work, let us consider CO_2 . The vibrationally resolved branching ratios and asymmetry parameters were obtained²¹ near a broad autoionizing resonance which is a member of a Rydberg series converging to the $B\ 2\Sigma^+$ state of the ion. An example of the vibrationally resolved PES near the resonance is shown in Fig. 8. The curve is a model fit to the data, with the intensity of each ionic vibrational level shown by a bar. Two features are especially noteworthy. The first is that the experimental vibrational progression does not follow the expected Franck-Condon progression. Secondly, the open bars in the figure represent the intensity of the three vibrational levels of the ν_2 progression ($n,1,0$) which is normally forbidden by selection rules. This progression had to be included to fit the data and its presence suggests that the resonance supplies the coupling required to mix the allowed and unallowed states. Fig. 9 is an illustration of the branching ratios obtained near the autoionizing resonance. Notice that the ($n,1,0$) progression only contributes to the ionization cross section in the vicinity of the resonance, and that the high vibrational levels of the ($n,0,0$) progression (denoted by remainder in Fig. 9) show a large intensity variation near the resonances at 16.5 and 16.6 eV. This strong non-Franck-Condon behavior is typical of the results obtained in many similar systems.

Soon, the present electron spectrometer will be replaced by a new one²² with higher resolution (20 meV typical) and 500 times greater sensitivity. This spectrometer will be an important tool for the detailed study of molecular dynamics in the VUV and soft x-ray spectral region.

Machine Improvements

Fig. 1 is an illustration of the rather dramatic improvement in spectral intensity, especially at short wavelengths, that has been obtained by raising the energy of the electrons in the storage ring from 250 MeV to 280 MeV. An energy of 300 MeV has been achieved but the beam lifetime becomes rather short due to insufficient r.f. accelerating voltage. However, a half-life of several hours is possible at 280 MeV. Two other improvements are in progress: one is a new r.f. cavity insertion so that the harmonic content of the r.f. field can be tailored to increase the phase space available to the electrons and further increase the beam lifetime; the second improvement is a modification of the injector r.f. cavity that will permit the injection and storage of larger circulating currents.

This brief report outlines only a few of the research problems that can be studied at a small dedicated low-energy facility with a high brightness beam that is tailor-made to exploit the spectral region between the carbon K edge and the visible.

Acknowledgments

This work is supported in part by the U.S. Department of Energy, the Office of Naval Research, the National Aeronautics and Space Administration and NATO Grant No. 1939.

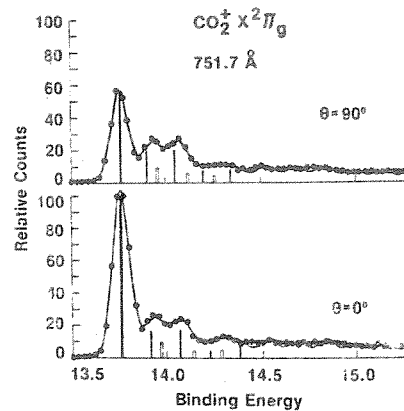


Fig. 8. Photoelectron spectra of CO_2 . The vertical scale is electron counts per unit energy per unit light flux. The heights are adjusted to 100 for the largest peak value. The solid bars represent the relative amplitude of the main ν_1 vibrational progression in the fit. The open bar represents the three vibrational levels of the form ($n,1,0$) of the ν_2 progression needed to fit the data.

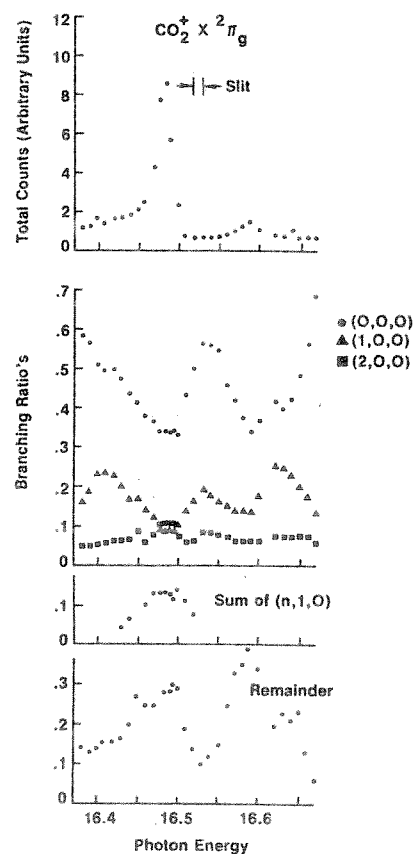


Fig. 9. The $\text{CO}_2^+ \times 2\Pi_g$ vibrational branching ratios and total electron count for the resonance in the 750\AA region. The branching ratios are the fraction of a given peak area to the total electron intensity in the 1.6 eV electron energy range spanned in Fig. 8. It should be noted from Fig. 8 that the photoelectron spectra do not go to zero at higher binding energies, indicating there are still other vibrational excitations ignored here. The designation ($0,0,0$) means $\nu_1=0$, $\nu_2=0$, $\nu_3=0$ for the state of the ion given. The sum ($n,1,0$) indicates the sum of the substructure where $n=1-3$. The remainder is the residual intensity not accounted for in the other designated curves.

References

1. A.C. Parr, Nucl. Inst. and Meth. 195, 7 (1982);
and A.C. Parr, G. Rakowsky, D.L. Ederer, R.L.
Stockbauer, J.B. West and J.L. Dehmer, IEEE
Transactions on Nuclear Science NS-28, 1210 (1981).
2. R. Stockbauer and R.P. Madden, Nucl. Inst. and
Meth. 195, 207 (1982).
3. E.B. Saloman, Nucl. Inst. and Meth. 172, 79 (1980).
4. D.L. Ederer, B.E. Cole and J.B. West, Nucl. Inst.
and Meth. 172, 185 (1980).
5. J. Schwinger, Phys. Rev. 75, 1912 (1949).
6. L.R. Hughey and A.R. Schaefer, Nucl. Inst. and
Meth. 195, 367 (1982).
7. E.B. Saloman, S.C. Ebner and L.R. Hughey, Optical
Engineering 21, 951 (1982).
8. J.A.R. Samson, J. Opt. Soc. Am. 54, 6 (1964).
9. J.C. Rife and J.F. Osantowski, SPIE Vol. 315,
"Reflecting Optics for Synchrotron Radiation"
p. 103 (1981).
10. T.E. Madey, F.P. Netzer, J.E. Houston, D.M. Hanson,
and R. Stockbauer, in Proceedings of DIET Workshop,
Springer-Verlag Series in Chemical Physics, eds.
N. Tolk, U. Traum, J. Tully and T. Madey, (Springer-
Verlag, New York, 1982).
11. R. Stockbauer, D.M. Hanson, S.A. Flodstrom, E.
Bertel and T.E. Madey, Phys. Rev. B26, 1885 (1982);
D.M. Hanson, R. Stockbauer, and T.E. Madey, J.
Chem. Phys. 77, 1569 (1982).
12. L.R. Hughey, R.T. Williams, J.C. Rife, D.J. Nagel
and M.C. Peckerer, Nucl. Inst. and Meth. 195, 267
(1982).
13. G. Mehlman, J.W. Cooper, and E.B. Saloman, Phys.
Rev. A25, 2113 (1982).
14. J.W. Cooper and E.B. Saloman, Phys. Rev. A26, 1452
(1982).
15. J.S. Foster, Proc. R. Soc. London 117, 137 (1928).
16. R.P. Madden and A.C. Parr, Appl. Opt. 21, 179
(1982).
17. K. Codling, A.C. Parr, D.L. Ederer, R. Stockbauer,
J.B. West, B.E. Cole and J.L. Dehmer, J. Phys. B:
14, 657 (1981).
18. A.C. Parr, D.L. Ederer, B.E. Cole, J.B. West, R.
Stockbauer, K. Codling and J.L. Dehmer, Phys. Rev.
Lett. 46, 22 (1981).
19. D.L. Ederer, A.C. Parr, B.E. Cole, R. Stockbauer,
J.L. Dehmer, J.B. West, and K. Codling, Proc. Roy.
Soc. Lond. A 378, 423 (1981).
20. J.L. Dehmer, A.C. Parr, S. Wallace and D. Dill,
to be published in Phys. Rev. A.
21. A.C. Parr, D.L. Ederer, J.L. Dehmer, D.M.P.
Holland, J. Chem. Phys. 77, 111 (1982).
22. A.C. Parr, S.H. Southworth, J.L. Dehmer and
D.M.P. Holland, to be published in Int. Journ.
Mass Spectrom. and Ion Phys.